Estimation of the Diffusion-Limited Rate of Microtubule Assembly

David J. Odde
Department of Chemical Engineering, Michigan Technological University, Houghton, Michigan 49931 USA

ABSTRACT Microtubule assembly is a complex process with individual microtubules alternating stochastically between extended periods of assembly and disassembly, a phenomenon known as dynamic instability. Since the discovery of dynamic instability, molecular models of assembly have generally assumed that tubulin incorporation into the microtubule lattice is primarily reaction-limited. Recently this assumption has been challenged and the importance of diffusion in microtubule assembly dynamics asserted on the basis of scaling arguments, with tubulin gradients predicted to extend over length scales exceeding a cell diameter, ~50 μm. To assess whether individual microtubules in vivo assemble at diffusion-limited rates and to predict the theoretical upper limit on the assembly rate, a steady-state mean-field model for the concentration of tubulin about a growing microtubule tip was developed. Using published parameter values for microtubule assembly in vivo (growth rate = 7 μm/min, diffusivity = 6×10^{-12} m^2/s, tubulin concentration = 10 μM), the model predicted that the tubulin concentration at the microtubule tip was ~89% of the concentration far from the tip, indicating that microtubule self-assembly is not diffusion-limited. Furthermore, the gradients extended less than ~50 nm (the equivalent of about two microtubule diameters) from the microtubule tip, a distance much less than a cell diameter. In addition, a general relation was developed to predict the diffusion-limited assembly rate from the diffusivity and bulk tubulin concentration. Using this relation, it was estimated that the maximum theoretical assembly rate is ~65 μm/min, above which tubulin can no longer diffuse rapidly enough to support faster growth.

GLOSSARY

c	concentration of tubulin (μM)
c_∞	concentration of tubulin far from microtubule (μM)
D	translational diffusivity (m^2/s)
K	conversion factor between V and W ($= 4.54 \times 10^{-17}$ μmol s^{-1} min μm^{-1})
N	number of protofilaments
r	radial position (nm)
s	distance from center of microtubule tip (nm)
s_o	radius of microtubule tip (nm)
V	microtubule growth rate (μm/min)
W	tubulin subunit incorporation rate (μmol/s)
z	axial position (nm)

INTRODUCTION

Microtubule assembly occurs by a phenomenon known as dynamic instability, in which individual microtubules switch stochastically between extended growth and shortening phases (Mitchison and Kirschner, 1984a,b). A single growth (or shortening) phase can result in the gain (or loss) of thousands of tubulin $\alpha\beta$-heterodimers, the protein complexes that constitute microtubules. Identifying the mechanisms responsible for dynamic instability is important not only for understanding how the cytoskeleton is regulated, but also for facilitating the development of microtubule-directed cancer chemotherapeutics (e.g., taxol and vinblastine), which are among the more effective anticancer drugs (Horwitz, 1994; Rowinsky et al., 1994; Wilson and Jordan, 1994).

Originally it was assumed that microtubule assembly dynamics could be modeled as a stochastic switching process without considering translational diffusion of tubulin subunits to the growing tip of the microtubule as a potentially rate-limiting effect (Hill, 1987; Mitchison and Kirschner, 1987; Bayley et al., 1989, 1990; Gliksman et al., 1993; Martin et al., 1993; Odde and Buettner, 1995; Odde et al., 1995). The basis for neglecting diffusion has been that tubulin can diffuse rapidly relative to the assembly rate (Bayley, 1993). Using a diffusivity of 5.9×10^{-12} m^2/s (tubulin in sea urchin eggs; Salmon et al., 1984) implies that in 1 s the average displacement of a tubulin subunit will be ~6 μm, whereas a microtubule will elongate only ~0.12 μm in the same time (assuming a growth rate of 7 μm/min; Cassimeris et al., 1988). In addition, Brownian dynamics simulation of protein-protein binding demonstrated that rotational diffusion during a lengthy collision between binding partners, and not translational diffusion, is most likely the rate-limiting step in association (Northrup and Erickson, 1992). Together these results support the assumption that translational diffusion can be neglected when microtubule dynamic instability is modeled.

However, in more recent studies this assumption has been challenged. First, by using a mean-field modeling approach that combined reaction and diffusion effects, it was found that microtubules nucleated from a planar surface divide into two populations: a leading group that has ample tubulin available for continued growth and a lagging group that exists in a region left tubulin-poor by the leading group (Dogterom and Leibler, 1993). It was asserted that this effect would take place as long as the spacing between microtubules was less than a characteristic distance, $l_d = D/V$, which for the parameters listed above is ~50 μm. This

Received for publication 21 October 1996 and in final form 26 March 1997.

Address reprint requests to Dr. David J. Odde, Department of Chemical Engineering, Michigan Technological University, Houghton, MI 49931. Tel.: 906-487-2140; Fax: 906-487-3213; E-mail: odde@mtu.edu.

0006-3495/97/07/88/09 $2.00

suggests that a microtubule will be directly affected by all of the other microtubules in the cell, because this distance exceeds typical cell dimensions. A subsequent study, again using mean-field analysis, concluded that diffusive effects could play a role in assembly when centrosome-nucleated microtubules are less than ~5 μm long (Dogterom et al., 1995). In addition to these theoretical analyses, it was shown that microtubules assembled in vitro at concentrations high enough to initiate spontaneous bulk nucleation and assembly exhibited birefringent patterns characteristic of nonlinear systems in which reaction and diffusion are tightly coupled (Tabony, 1994). Given the complex, interactive nature of these systems, in which tubulin diffusion has been implicated as an important aspect of microtubule assembly, it would be useful to be able to predict the theoretical upper limit for the assembly rate and define the conditions under which individual microtubule assembly will be diffusion-limited.

To address these issues, I developed a mean-field model to predict the tubulin concentration as a function of distance from the microtubule tip. Using a GTP-tubulin concentration of 10 μM (Mitchison and Kirschner, 1987), a growth rate of 7 μm/min, and a diffusivity of 5.9×10^{-12} m^2/s, it was found that the surface concentration is ~8.9 μM and that the concentration gradient decays to background levels within ~50 nm of the tip. In addition, an expression for the theoretical maximum growth rate was derived and used to estimate a ~65 μm/min maximum growth rate, assuming the same tubulin concentration and diffusivity. Using the mean-field approach, a model was also obtained for the GDP-tubulin distribution during disassembly. The model is sufficiently general that it can be applied to other linear polymers such as filamentous actin.

MODEL

The starting point in the analysis is to define the equation of continuity for tubulin and the relevant boundary conditions for the system. Assuming Fick's law of diffusion, the steady-state transport equation for cylindrical coordinates is given by

$$0 = D\left(\frac{1}{r}\frac{\partial}{\partial r}\left(r\frac{\partial c}{\partial r}\right) + \frac{\partial^2 c}{\partial z^2}\right) - V\frac{\partial c}{\partial z} \tag{1}$$

where c is the concentration of tubulin, z is the axial position (assumed to be the axis of the microtubule), r is the radial position (away from the microtubule axis), D is the translational diffusivity of tubulin, and V is the rate of growth. The growing tip of the microtubule is fixed at the origin, and therefore the medium can be regarded as plug flow past the growing tip, which gives rise to the convection term in Eq. 1, because the microtubule continues to grow (at rate V) through the stagnant medium. To solve for $c(r, z)$, a new variable, s, was defined as the distance from the origin:

$$s = \sqrt{r^2 + z^2} \tag{2}$$

The appropriate boundary conditions for the system are

$$\text{B.C. 1} \quad c = c_\infty \quad \text{at } s = \infty \tag{3A}$$

$$\text{B.C. 2} \quad 4\pi s^2 D\left(\frac{\partial c}{\partial s}\right)_z = W \quad \text{at } s = s_0 \tag{3B}$$

$$\text{B.C. 3} \quad \left(\frac{\partial c}{\partial r}\right)_z = 0 \quad \text{at } r = 0 \tag{3C}$$

where s_0 is the radius of the tip (see below) and W is the rate of subunit incorporation in μmol s^{-1}. Note that the rate of subunit incorporation (W) is proportional to the growth rate (V) according to the relation $W \equiv KV$, where K is a constant ($K = 4.54 \times 10^{-17}$ μmol s^{-1} min μm^{-1}, assuming 1640 subunits/μm of microtubule length). The first boundary condition (Eq. 3A) specifies the bulk concentration of tubulin (assumed constant), the second boundary condition (Eq. 3B) specifies a constant flux at the surface of the microtubule tip, and the third boundary condition (Eq. 3C) imposes the required symmetry about the z axis. To obtain an analytical solution, it was necessary to model the microtubule tip as a sphere with surface area equal to the surface area of a growing microtubule tip. Thus the final expression for the steady-state tubulin concentration is given by

$$c(r, z) = c_\infty - \frac{W}{4\pi Ds}\exp\left[-\frac{V}{2D}(s - z)\right] \tag{4}$$

This solution has three parameters: the diffusivity D, the bulk tubulin concentration c_∞, and the growth rate V (which is proportional to W). A related expression is obtained for the case of microtubule disassembly, in which the GDP-tubulin concentration is given by

$$c(r, z) = \frac{W}{4\pi Ds}\exp\left[-\frac{V}{2D}(s - z)\right] \tag{5}$$

which is obtained by setting the bulk concentration to zero in Eq. 3A and reversing the sign of the flux expression in Eq. 3B. Symmetry about the z axis is again required by Eq. 3C. Given the appropriate parameters, the expressions in Eqs. 4 and 5 can be used to predict the steady-state concentration profiles about growing and shortening microtubules, respectively. The model does not make any particular assumption about the polymerization process, only that it can be characterized by a constant growth rate and a single translational diffusivity. Therefore, the equations are sufficiently general to be applied to an arbitrary linear polymerization or depolymerization process.

RESULTS

Predicted tubulin concentration profile during assembly

To determine whether there is a significant depletion of tubulin in the vicinity of a growing microtubule tip, pub-

lished values for the rates of diffusion and reaction were used as model parameter estimates. As a basic parameter set, $V = 7$ μm/min (measured in newt lung epithelial cells; Cassimeris et al., 1988), $D = 5.9 \times 10^{-12}$ m^2/s (measured in sea urchin eggs; Salmon et al., 1984), and $c_\infty = 10$ μM (estimated for interphase fibroblasts; Mitchison and Kirschner, 1987) were chosen. When these parameters are used in Eq. 4, the concentration at the microtubule surface is ~8.9 μM and the concentration returns to the bulk concentration level (10 μM) within ~50 nm of the tip surface, as shown in Fig. 1. Because the surface concentration is only ~10% less than the bulk concentration, the assembly is well below the diffusion-limited rate that occurs when the surface concentration reaches zero (at which point the subunits react instantaneously at the microtubule tip).

An interesting feature of the concentration profile is that it is apparently dependent only on the distance, s, from the tip. By examining Eq. 4, it can be seen that the exponential term, which gives rise to asymmetry in the concentration profile, is very nearly unity for the parameters used here (the exponential decay constant $V/2D = 9.9 \times 10^{-6}$ nm^{-1}). In addition, using the Frössling correlation for flow past a sphere predicts a Sherwood number of 2.001, essentially equal to the limiting value of 2 for stagnant systems (McCabe et al., 1993). Therefore a simplified form of Eq. 4 is given by

$$c(s) = c_\infty - \frac{W}{4\pi D s} \tag{6}$$

where the concentration is now only a function of the distance, s, from the tip. For the basic parameter set, the radius of the tip, s_o, was estimated by assuming that the surface area of a protofilament tip is ~16 nm^2 (approximately a 4 nm × 4 nm surface). By using a 13-protofilament microtubule, an effective surface area of 13 × 16 nm^2 = 208 nm^2 is obtained, which corresponds to a sphere of radius $s_o = 4$ nm. The effect of varying the number of sites available for tubulin incorporation is discussed below.

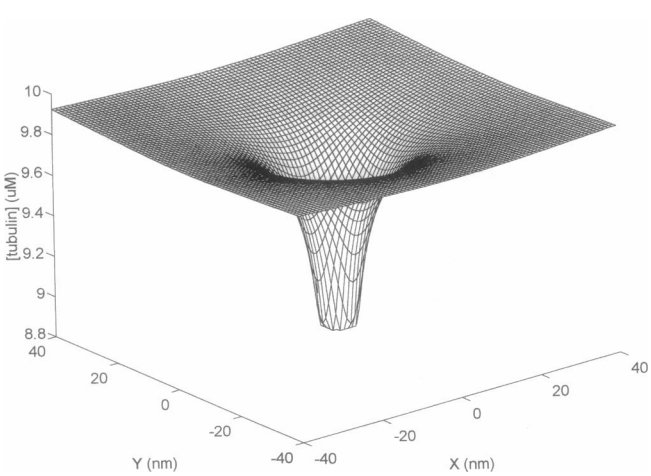

FIGURE 1 Predicted steady-state GTP-tubulin concentration profile about a growing microtubule. The basic parameter set ($V = 7$ μm/min, $D = 5.9 \times 10^{-12}$ m^2/s, $c_\infty = 10$ μM) was used, and the tip was modeled as a sphere with radius 4 nm. The concentration at the tip is ~8.9 μM, and the concentration gradient occurs over ~50 nm distance from the tip. The microtubule lies in the horizontal plane parallel to the x axis, with the tip centered at the origin. Distances (on the *horizontal axes*) are in nanometers and concentration (on the *vertical axis*) is in micromolarity.

Effect of growth rate

Cells are capable of regulating their rate of microtubule assembly, for example, by increasing the assembly rate in mitosis severalfold over the interphase assembly rate (Belmont et al., 1990; Hayden et al., 1990; Simon et al., 1992). The effect of growth rate on the tubulin concentration profile is shown in Fig. 2. When the basic parameter set is used, the concentration again reaches the bulk level (10 μM) within ~50 nm, although the gradient extends to greater distances as the velocity increases. In addition, the surface concentration does not reach zero until the growth rate reaches 65 μm/min, much higher than the highest measured value of 20 μm/min in Chinese hamster ovary (CHO) fibroblast cells (Shelden and Wadsworth, 1993). Note that when the surface concentration is zero, the bulk concentration is c_∞ and therefore the tubulin concentration is still above the critical concentration required to support microtubule assembly. When the 20 μm/min growth rate is used, an intermediate concentration profile is obtained between the basic parameter rate and the diffusion-limited assembly rate, and the tip concentration in this case is ~6.9 μM.

Effect of diffusivity

With the experimentally determined diffusivity (5.9×10^{-12} m^2/s in sea urchin eggs), the tip concentration is

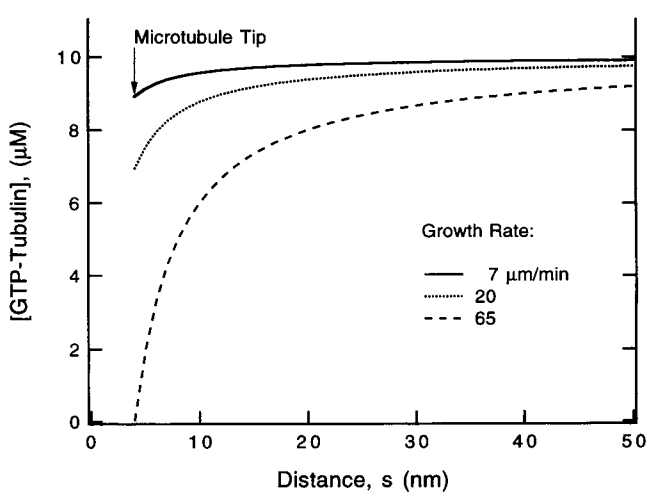

FIGURE 2 Effect of velocity on predicted GTP-tubulin concentration profile. Using the basic parameter set, the growth becomes diffusion-limited when the velocity reaches 65 μm/min, because at this point the concentration at the tip is zero. The highest reported growth rate is 20 μm/min, which is shown for comparison.

predicted to be 8.9 μM. However, in the cell the effective diffusivity can potentially depend on the local structure of the cytoplasm (Provance et al., 1993), and therefore it is useful to know how the assembly will be affected when the diffusivity is decreased. As shown in Fig. 3, the tip concentration decreases with decreasing diffusivity and reaches zero (i.e., the diffusion limit) when the diffusivity is 6.4×10^{-13} m^2/s, which is ninefold lower than that measured by Salmon et al. (1984). Again, the tubulin concentration gradient exists only over ~50 nm.

Upper limit for microtubule assembly rate

The theoretical maximum growth rate can be obtained from Eq. 4 by setting c to zero and solving for V. Assuming that the exponential goes to unity as discussed above, we obtain

$$V_{max} = \frac{4\pi D c_\infty s_0}{K} \tag{7}$$

where K is the conversion factor between the velocity, V, and the rate of subunit incorporation, W. This result implies a linear relationship between diffusivity and maximum velocity, as shown in Fig. 4. In the region below the line, assembly is physically possible, whereas above the line diffusion is not sufficiently rapid to sustain the required growth rate. For example, by using the basic parameter set ($V = 7$ μm/min, $D = 5.9 \times 10^{-12}$ m^2/s), a point on the graph is defined that is well below the diffusion-limited maximum growth rate of 65 μm/min for this basic parameter set. The limiting line in Fig. 4 has a slope that is directly proportional to the bulk concentration, and therefore doubling the tubulin concentration effectively doubles the maximum growth rate. In general, the relation given in Eq. 7 provides a map of the parameter space and serves to define how "close" the system is to the diffusion limit.

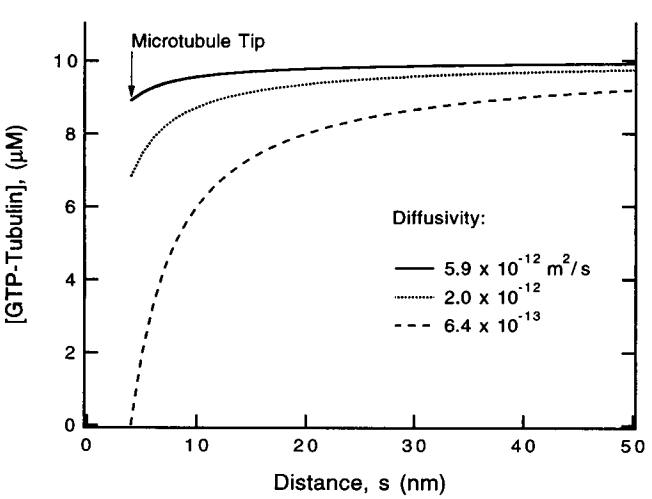

FIGURE 3 Effect of diffusivity on the predicted GTP-tubulin concentration profile. Using the basic parameter set, growth becomes diffusion-limited when the diffusivity reaches 6.4×10^{-13} m^2/s. An intermediate diffusivity of 2.0×10^{-12} m^2/s is shown for comparison.

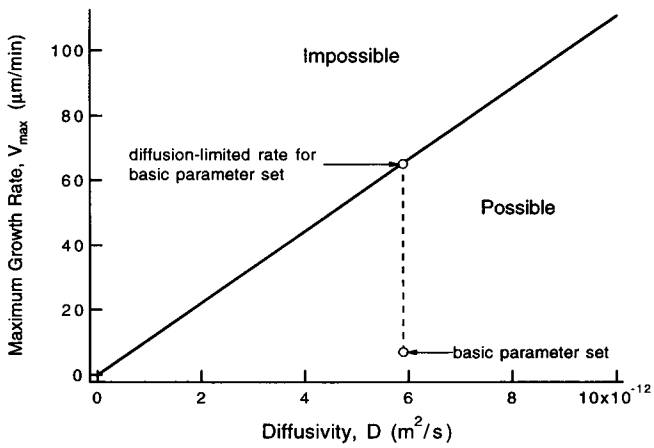

FIGURE 4 Predicted upper limit for microtubule growth rate. The maximum rate, V_{max}, is a linear function of D according to Eq. 6. Velocities below the maximum are physically possible, whereas those above the limit are not. When the basic parameter set is used, all reported velocities fall below the line and are at least a factor of 2–3, and more typically a factor of ~10, below the diffusion-limited velocity.

Effect of number of protofilament sites available for subunit incorporation

In the model development, the microtubule tip was approximated as a sphere of radius s_o. To determine s_o, the area of the microtubule tip was estimated and a sphere of equal surface area used in the calculations ($s_o = 4$ nm). To make this estimate it was assumed that all 13 protofilaments were capable of having subunits added to their termini. However, electron microscopic images of microtubule tips indicate that protofilaments grow in a concerted fashion, suggesting that not all protofilaments are capable of having subunits added at all times (Simon and Salmon, 1990; Mandelkow et al., 1991; Chrétien et al., 1995). In addition, microtubules can have variable numbers of protofilaments instead of the nominal 13 assumed in the basic parameter set. Thus it is necessary to relate s_o to the number of sites available for addition. This relationship is given by

$$s_o = 2\sqrt{\frac{N}{\pi}}\,(\text{nm}) \tag{8}$$

where N is the number of sites available for addition, and a 16-nm^2 area is assumed for each site (see description in Model section above). As shown in Fig. 5, by combining Eqs. 7 and 8, the maximum growth rate can be estimated as a function of the number of protofilaments that are capable of adding a tubulin subunit. Using $N = 1$, the lowest possible value, yields a diffusion-limited growth rate of 18 μm/min, roughly equal to the fastest reported growth rate (~20 μm/min), but still above the basic parameter set rate of $V = 7$ μm/min.

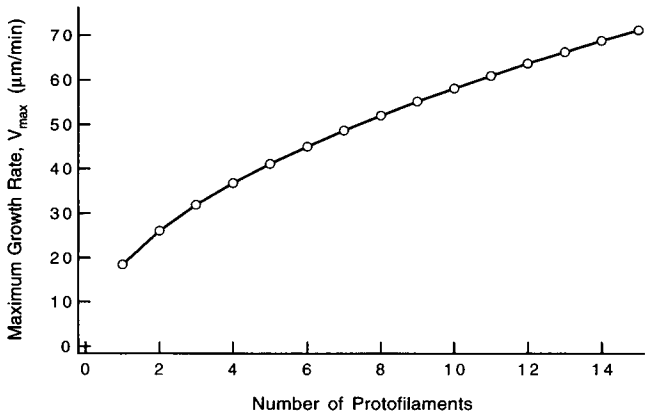

FIGURE 5 Maximum growth rate as a function of number of sites available for subunit addition. To predict the diffusion-limited growth rate, it was assumed that 13 sites were available for subunit addition, corresponding to a 65 μm/min growth rate. Even in the extreme of only one site being available, the basic growth rate of 7 μm/min is still predicted to be below the diffusion limit of ~18 μm/min.

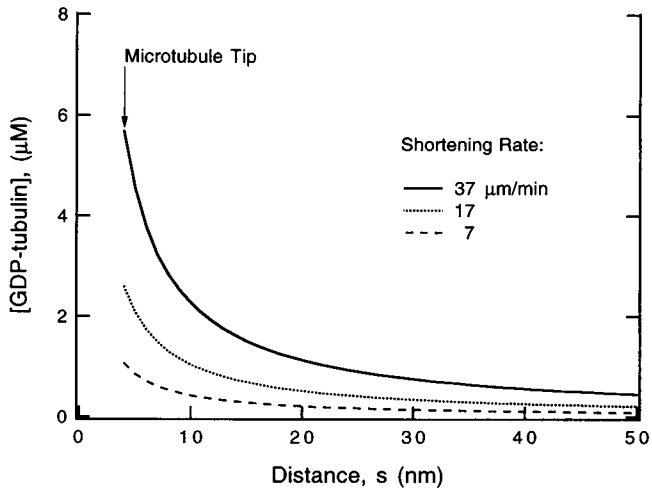

FIGURE 6 Predicted steady-state GDP-tubulin concentration profile during disassembly. After incorporation into the microtubule lattice, GTP-tubulin undergoes hydrolysis to GDP-tubulin. When the microtubule switches into the shrinkage state, GDP-tubulin is released from the microtubule tip. A shrinkage rate of 17 μm/min, measured in newt lung epithelial cells (Cassimeris et al., 1988), is typical of in vivo shrinkage rates. Note that increasing disassembly rates lead to higher GDP-tubulin concentrations at the tip.

GDP-tubulin concentration profiles during disassembly

The basic model (Eq. 4) can be modified to describe the concentration profile of tubulin during disassembly (Eq. 5). Although tubulin is incorporated into the lattice as GTP-tubulin, it leaves the lattice as GDP-tubulin because of the GTP hydrolysis associated with dynamic instability (Carlier and Pantaloni, 1981; Carlier, 1982; O'Brien et al., 1987). Assuming that V = 17 μm/min (measured for newt lung epithelial cells; Cassimeris et al., 1988) and c_∞ = 0 μM, the model predicts a tip concentration of 2.6 μM, with the gradient vanishing within ~50 nm of the tip, as shown in Fig. 6. Higher disassembly rates lead to higher tip concentrations. The parameter values used cover the reported range of shortening rates (see summaries in Gildersleeve et al., 1992; Odde and Buettner, 1995). These concentrations are sufficiently large that they could influence microtubule disassembly and cause occasional pauses during shrinkage phases (Vandecandelaere et al., 1995).

DISCUSSION

By modeling the growing microtubule tip as a sphere moving at rate V through a medium having tubulin concentration c_∞ and a tubulin diffusivity D, an analytical solution was obtained for the steady-state diffusion-reaction problem. When literature values are used for these parameters, the concentration of tubulin at the growing tip is estimated to be ~89% of the bulk concentration, c_∞. If the ratio of V/D is increased ninefold, then the microtubule growth is at the diffusion limit, implying that microtubules are normally assembled at rates well below the diffusion limit. In addition, the concentration gradient generated by assembly extends only ~50 nm from the tip, thus limiting the distance over which a single microtubule can exert its influence over the assembly of other microtubules by depleting the local tubulin pool.

Limitations of the model

The model currently assumes that the microtubule tip can be represented as a sphere of surface area equal to that of the microtubule tip. Doing so permits an analytical solution to the model, and the challenge then is to estimate the appropriate size for the sphere. It was assumed that 13 protofilaments are capable of tubulin subunit addition and that, if the surface area of each addition site can be modeled as a 4 nm × 4 nm square, there is a total surface area of 208 nm^2, which corresponds to a 4-nm spherical radius. Based on electron microscopic images of growing microtubules, it appears that protofilaments remain concerted in their growth, so that very few project far out in front of the rest (Simon and Salmon, 1990; Mandelkow et al., 1991; Chrétien et al., 1995). This suggests that protofilaments are not always capable of subunit addition (Chen and Hill, 1985; Bayley et al., 1990) and that the surface area available for growth is therefore reduced, resulting in a spherical radius of less than 4 nm (see Fig. 5). However, the outer radius of a microtubule is ~13 nm, and using much smaller radii (<4 nm) may place a physically unrealistic constraint on the assembly. For now, it seems reasonable to base the size on 13 protofilaments until experimental evidence permits better estimation of the surface area available for growth. It should be noted that even using a 1-nm radius (corresponding to a single protofilament) gives a diffusion-limited growth rate of 18 μm/min, roughly a factor of 2–3 above the growth rate measured in newt lung cells. In addition, the

model ignores the excluded volume of the microtubule itself, the presence of which would presumably favor assembly and therefore a higher upper limit (Zimmerman and Minton, 1993). More realistic models for the tip surface will require numerical solutions to the transport problem.

Another limitation of the model is that it is a mean-field solution. Therefore the stochastic fluctuations in growth rate, diffusivity, and bulk tubulin concentration are not accounted for in the model and are instead averaged over time and space to obtain the steady-state solution. For example, it has been shown for microtubules assembled in vitro from purified tubulin that the growth rate can exhibit significant fluctuations beyond that attributable to measurement error (Gildersleeve et al., 1992; Odde et al., 1996). Therefore, during a transiently accelerated growth period, a growing microtubule may reach the diffusion limit. However, it would be expected that the transient depletion of tubulin would tend to slow the growth, thus restoring the velocity toward its average rate. Because microtubules persist in their growth for extended periods (on the order of a minute) and exhibit roughly constant growth, the mean-field assumption can be a useful approximation. It is worth noting that, based on the data of Gildersleeve et al., the experimentally observed fluctuations in growth rate (SD/mean = 0.23 for ~20-s periods) are much larger than is predicted based on the assumption of Poisson arrivals of tubulin dimers (SD/mean = 0.025) or experimental error (SD/mean = 0.07). This suggests that the experimentally observed fluctuations are more likely the result of GTP-cap dynamics in the microtubule lattice as predicted by computer simulations (Martin et al., 1993; Odde et al., 1996).

Comparison to experiment

The growth rate for microtubules can vary, depending on the conditions (reviewed in Cassimeris, 1993; see also tabulation of reported values in Gildersleeve et al., 1992; Odde and Buettner, 1995). In purified systems in vitro, the growth rates are typically ~1 μm/min, whereas in living cells they are typically 4–7 μm/min. Higher rates of 10–12 μm/min have been observed in *Xenopus* egg extracts (Belmont et al., 1990; Verde et al., 1992), and a rate of 20 μm/min has been measured for CHO fibroblasts (Shelden and Wadsworth, 1993). In CHO fibroblasts, the standard deviation was 10 μm/min (N = 25), indicating that a subset of microtubules elongates at even higher rates (~30 μm/min). Because the diffusion limit is predicted to be ~65 μm/min using the basic parameter set, the highest reported rates are still at least a factor of 2 below the diffusion limit. That assembly is generally below the diffusion limit has implications for understanding the mechanisms of the microtubule-associated protein XMAP215 (and other molecules having similar activity), which accelerates microtubule elongation from 1 μm/min to 8 μm/min in a purified assembly system (Vasquez et al., 1994). The present model predictions suggest that XMAP215 acts not to promote tubulin transport as originally suggested by Vasquez et al., but rather to promote the incorporation of tubulin subunits into the microtubule lattice structure, perhaps by facilitating the proper orientation of tubulin at the microtubule tip.

Whereas data abound for microtubule growth rates, only two studies have reported on the diffusivity of tubulin in the cytoplasm (Salmon et al., 1984; Salmon and Wadsworth, 1986). Using sea urchin eggs microinjected with fluorescein-tubulin, fluorescence redistribution after photobleaching (FRAP) was performed, and, using Fick's law of diffusion, a translational diffusivity of $D = 5.9 \pm 2.2 \times 10^{-12}$ m^2/s was estimated. Salmon and Wadsworth (1986) measured the diffusivity of tubulin in BSC-1 cells using FRAP and estimated that $D = 1\text{–}2 \times 10^{-12}$ m^2/s (at a temperature of 32°C). Using the lower value of $D = 1 \times 10^{-12}$ m^2/s corresponds to a maximum growth rate of 11 μm/min, whereas Schulze and Kirschner measured the growth rate in BSC-1 cells to be 5.0 ± 2.4 μm/min (Schulze and Kirschner, 1988). Salmon et al. (1984) estimated that the apparent viscosity of the egg cytoplasm was about eight times that of water. Similarly, for fluorescent dextrans of approximately the same size as tubulin, the ratio of viscosities (cytoplasm to water) was ~6 in Swiss 3T3 cells (Luby-Phelps et al., 1986). In a study of tubulin transport in growing grasshopper nerve axons, the diffusivity of a fluorescent dextran expected to have diffusion characteristics similar to those of tubulin (based on size) was estimated to be $D = 8.0 \pm 1.1 \times 10^{-12}$ m^2/s in the axon (Sabry et al., 1995). That tubulin diffusivities are generally lower in the cytoplasm than in aqueous solution may reflect weak, transient binding of tubulin to larger (possibly tubulin and/or MAP oligomeric) structures (Jacobson and Wojcieszyn, 1984) and/or an excluded volume effect due to macromolecular crowding in the cytoplasm (Zimmerman and Minton, 1993). For in vitro high-resolution microscopy experiments with purified tubulin, in which D is about eightfold higher than in sea urchin egg cytoplasm and V is ~1 μm/min, microtubule assembly occurs at a rate ~520-fold below the diffusion-limited rate. Therefore, even though these experiments are typically conducted with microtubules assembled close to a glass coverslip (within a few hundred nanometers) to facilitate visualization, it is very unlikely that the nearby glass barrier restricts access to tubulin dimers. Clearly, more in vivo data are needed, particularly to determine if substructures of the cytoplasm, such as the actin cortex or kinetochores, are especially restrictive of tubulin diffusion.

Comparison to previous theoretical analysis

Previous mathematical modeling of diffusion and reaction in microtubule assembly concluded that microtubules can interact with each other via tubulin gradients as long as microtubules are separated by a distance less than a characteristic diffusion length given by $l_d = D/V$, which for the basic parameter set used here is ~50 μm (Dogterom and Leibler, 1993). This criterion is inconsistent with the present

model results, in which tubulin gradients about single microtubules extend over a distance of less than ~50 nm. The Dogterom and Leibler model differs from the present model in that it models microtubule populations undergoing dynamic instability (the two-state assembly dynamics characteristic of microtubules), whereas the present model, of single microtubules undergoing growth, is designed only to estimate the theoretical upper limits for the assembly rate of single microtubules. Although the present model does not consider the gradients when multiple microtubules are present, it seems highly unlikely that interactions would occur over distances as large as 50 μm. Subsequent analysis by Dogterom and co-workers reconsidered the situation of diffusion and reaction for microtubules nucleated from centrosomes. They retracted their earlier scaling criterion (l_d) and concluded that if there are more than 10–1000 microtubules, then diffusion cannot be neglected a priori (Dogterom et al., 1995). Using the 1-μm centrosomal radius assumed in their analysis, the average spacing between microtubules at the centrosomal surface will be ~1000 nm for 10 microtubules and ~100 nm for 1000 microtubules (with the spacing increasing linearly with radial distance), which is roughly consistent with the 50-nm distance obtained in the present analysis for single microtubule gradients (considering that the present model is only for single microtubules). In addition to the immediate vicinity of the centrosome, microtubules can also be closely spaced in kinetochores (~50–60 nm; Rieder, 1982) and in axons (~75 nm; Yamada et al., 1971), and therefore diffusion would be expected to play a more prominent role in these specialized structures. However, given that microtubules in the cell are typically separated by distances much larger than 50 nm, it seems likely that most microtubules in vivo are not diffusion-limited in their growth. In addition, both α-tubulin synthesis and β-tubulin synthesis are autoregulated such that decreased free tubulin levels promote new tubulin synthesis (Ben-Ze'ev et al., 1979; Cleveland et al., 1981; Gonzalez-Garay and Cabral, 1996). Thus any persistent gradients would tend to be offset to some extent by increased synthesis.

Role of diffusion in dynamic instability

Even though single microtubule assembly is not predicted by the model to be diffusion-limited, diffusion could play a role in modulating the transition frequencies of dynamic instability. Microtubule growth is believed to be mediated by the presence of a stabilizing cap of GTP-tubulin subunits (reviewed in Bayley, 1990; Carlier, 1991; Erickson and O'Brien, 1992), and it has been shown that increased GTP-tubulin concentration reduces the frequency of the growth to shrinkage transition ("catastrophe"), suggesting that GTP-tubulin availability plays a role in this transition process (Walker et al., 1988; Martin et al., 1993). In addition, microtubules are temperature-sensitive and tend to disassemble when cooled to near freezing. This phenomenon could be explained, at least in part, by a decreased diffusivity, which would make a transient lack of GTP-tubulin occur more frequently. When microtubules are cooled from 37°C to 4°C, it is estimated (based on the Stokes-Einstein relation and the temperature dependence of the viscosity of water) that the diffusivity would decrease by a factor of ~2.5. Although this would not cause the growth to become diffusion-limited, it could cause more frequent periods of inadequate GTP-tubulin supply for continued microtubule growth, thus leading to more frequent catastrophes. Given that net microtubule assembly is a competition between assembly and disassembly, a small increase in the catastrophe frequency could cause a phase transition in the system by pushing it below its so-called critical concentration for microtubule assembly (Hill, 1987; Fygenson et al., 1994). In this regard it would be interesting to determine whether the diffusivity has an effect on the catastrophe frequency, even under conditions where growth is not expected to be diffusion-limited. In addition, the predicted concentrations of GDP-tubulin during disassembly are sufficiently high that they might be expected to play a role in GDP-tubulin-mediated pauses observed during microtubule disassembly (Vandecandelaere et al., 1995). This type of diffusive interaction could therefore play a role in the synchronous microtubule-mediated movement of chromosomes during prometaphase, a phenomenon known as directional instability (Skibbens et al., 1993).

In dividing eukaryotic cells, microtubules connect chromosomes to each of two spindle poles on either side of the chromosomes. One set of microtubules assembles synchronously on one side of a chromosome while the other set of microtubules disassembles synchronously on the other side. Directional instability is where the chromosome switches direction stochastically, much like dynamic instability, with the concomitant switching of assembly and disassembly states of all the microtubules. The mechanism by which directional instability occurs is not known. Based on the present analysis, the disassembling bundle on one side of the chromosome should have a substantially increased local concentration of GDP-tubulin, which would in turn support the continued disassembly of microtubules on the side where disassembly is occurring and provide a means of "communication" between adjacent microtubules.

I thank Lynne Cassimeris, Harold Erickson, and Mark Riley for critical comments on a draft version of the manuscript.

REFERENCES

Bayley, P. M. 1990. What makes microtubules dynamic? *J. Cell Sci.* 95:329–334.

Bayley, P. 1993. Why microtubules grow and shrink. *Nature.* 363:309.

Bayley, P. M., M. J. Schilstra, and S. R. Martin. 1989. A simple formulation of microtubule dynamics: quantitative implications of the dynamic

instability of microtubule populations in vivo and in vitro. *J. Cell Sci.* 93:241–254.

Bayley, P. M., M. J. Schilstra, and S. R. Martin. 1990. Microtubule dynamic instability: numerical simulation of microtubule transition properties using a lateral cap model. *J. Cell Sci.* 95:33–48.

Belmont, L. D., A. A. Hyman, K. E. Sawin, and T. J. Mitchison. 1990. Real-time visualization of cell cycle-dependent changes in microtubule dynamics in cytoplasmic extracts. *Cell.* 62:579–589.

Ben-Ze'ev, A., S. R. Farmer, and S. Penman. 1979. Mechanisms of regulating tubulin synthesis in cultured mammalian cells. *Cell.* 17: 319–325.

Carlier, M. 1991. Nucleotide hydrolysis in cytoskeletal assembly. *Curr. Opin. Cell Biol.* 3:12–17.

Carlier, M.-F. 1982. Guanosine-5′-triphosphate hydrolysis and tubulin polymerization. *Mol. Cell. Biochem.* 47:97–113.

Carlier, M.-F., and D. Pantaloni. 1981. Kinetic analysis of guanosine 5′-triphosphate hydrolysis associated with tubulin polymerization. *Biochemistry.* 20:1918–1924.

Cassimeris, L. 1993. Regulation of microtubule dynamic instability. *Cell Motil. Cytoskel.* 26:275–281.

Cassimeris, L., N. K. Pryer, and E. D. Salmon. 1988. Real-time observations of microtubule dynamic instability in living cells. *J. Cell Biol.* 107:2223–2231.

Chen, Y., and T. L. Hill. 1985. Monte Carlo study of the GTP cap in a five-start helix model of a microtubule. *Proc. Natl. Acad. Sci. USA.* 82:1131–1135.

Chrétien, D., S. D. Fuller, and E. Karsenti. 1995. Structure of growing microtubule ends: two-dimensional sheets close into tubes at variable rates. *J. Cell Biol.* 129:1311–1328.

Cleveland, D. W., M. A. Lopata, P. Sherline, and M. W. Kirschner. 1981. Unpolymerized tubulin modulates the level of tubulin mRNAs. *Cell.* 25:537–546.

Dogterom, M., and S. Leibler. 1993. Physical aspects of the growth and regulation of microtubule structures. *Phys. Rev. Lett.* 70:1347–1350.

Dogterom, M., A. C. Maggs, and S. Leibler. 1995. Diffusion and formation of microtubule asters: physical processes versus biochemical regulation. *Proc. Natl. Acad. Sci. USA.* 92:6683–6688.

Erickson, H. P., and E. T. O'Brien. 1992. Microtubule dynamic instability and GTP hydrolysis. *Annu. Rev. Biophys. Biomol. Struct.* 21:145–166.

Fygenson, D. K., E. Braun, and A. Libchaber. 1994. Phase diagram of microtubules. *Phys. Rev. E.* 50:1579–1588.

Gildersleeve, R. F., A. R. Cross, K. E. Cullen, A. P. Fagen, and R. C. Williams, Jr. 1992. Microtubules grow and shorten at intrinsically variable rates. *J. Biol. Chem.* 267:7995–8006.

Gliksman, N. R., R. V. Skibbens, and E. D. Salmon. 1993. How the transition frequencies of microtubule dynamic instability (nucleation, catastrophe, and rescue) regulate microtubule dynamics in interphase and mitosis: analysis using a Monte Carlo computer simulation. *Mol. Biol. Cell.* 4:1035–1050.

Gonzalez-Garay, M. L., and F. Cabral. 1996. Alpha-tubulin limits its own synthesis: evidence for a mechanism involving translational repression. *J. Cell Biol.* 135:1525–1534.

Hayden, J. H., S. S. Bowser, and C. L. Rieder. 1990. Kinetochores capture astral microtubules during chromosome attachment to the mitotic spindle: direct visualization in live newt lung cells. *J. Cell Biol.* 111: 1039–1045.

Hill, T. L. 1987. Linear Aggregation Theory in Cell Biology. Springer-Verlag, New York.

Horwitz, S. B. 1994. TAXOL (paclitaxel): mechanisms of action. *Ann. Oncol.* 5:S3–S6.

Jacobson, K., and J. Wojcieszyn. 1984. The translational mobility of substances within the cytoplasmic matrix. *Proc. Natl. Acad. Sci. USA.* 81:6747–6751.

Luby-Phelps, K., D. L. Taylor, and F. Lanni. 1986. Probing the structure of cytoplasm. *J. Cell Biol.* 102:2015–2022.

Mandelkow, E.-M., E. Mandelkow, and R. A. Milligan. 1991. Microtubule dynamics and microtubule caps: a time-resolved cryo-electron microscopy study. *J. Cell Biol.* 114:977–991.

Martin, S. R., M. J. Schilstra, and P. M. Bayley. 1993. Dynamic instability of microtubules: Monte Carlo simulation and application to different types of microtubule lattice. *Biophys. J.* 65:578–596.

McCabe, W. L., J. C. Smith, and P. Harriot. 1993. Unit Operations of Chemical Engineering, 5th Ed. McGraw-Hill, New York.

Mitchison, T., and M. Kirschner. 1984a. Microtubule assembly nucleated by isolated centrosomes. *Nature.* 312:232–237.

Mitchison, T. J., and M. W. Kirschner. 1984b. Dynamic instability of microtubule growth. *Nature.* 312:237–242.

Mitchison, T. J., and M. W. Kirschner. 1987. Some thoughts on the partitioning of tubulin between monomer and polymer under conditions of dynamic instability. *Cell Biophys.* 11:35–55.

Northrup, S. H., and H. P. Erickson. 1992. Kinetics of protein-protein association explained by Brownian dynamics computer simulation. *Proc. Natl. Acad. Sci. USA.* 89:3338–3342.

O'Brien, E. T., W. A. Voter, and H. P. Erickson. 1987. GTP hydrolysis during microtubule assembly. *Biochemistry.* 26:4148–4156.

Odde, D. J., and H. M. Buettner. 1995. Time series characterization of simulated microtubule dynamics in the nerve growth cone. *Ann. Biomed. Eng.* 23:268–286.

Odde, D. J., L. Cassimeris, and H. M. Buettner. 1995. Kinetics of microtubule catastrophe assessed by probabilistic analysis. *Biophys. J.* 69: 796–802.

Odde, D. J., L. Cassimeris, and H. M. Buettner. 1996. Spectral analysis of microtubule assembly dynamics. *AIChE J.* 42:1434–1442.

Provance, D. W., Jr., A. McDowall, M. Marko, and K. Luby-Phelps. 1993. Cytoarchitecture of size-excluding compartments in living cells. *J. Cell Sci.* 106:565–578.

Rieder, C. L. 1982. The formation, structure, and composition of the mammalian kinetochore and kinetochore fiber. *Int. Rev. Cytol.* 79:1–58.

Rowinsky, E. K., M. Wright, B. Monsarrat, and R. C. Donehower. 1994. Clinical pharmacology and metabolism of TAXOL (paclitaxel): update 1993. *Ann. Oncol.* 5:S7–S16.

Sabry, J., T. P. O'Connor, and M. W. Kirschner. 1995. Axonal transport of tubulin in Ti1 pioneer neurons in situ. *Neuron.* 14:1247–1256.

Salmon, E. D., W. M. Saxton, R. J. Leslie, M. L. Karow, and J. R. McIntosh. 1984. Diffusion coefficient of fluorescein-labeled tubulin in the cytoplasm of embryonic cells of a sea urchin: video image analysis of fluorescence redistribution after photobleaching. *J. Cell Biol.* 99: 2157–2164.

Salmon, E. D., and P. Wadsworth. 1986. Fluorescence studies of tubulin and microtubule dynamics in living cells. *In* Applications of Fluorescence in the Biomedical Sciences. D. L. Taylor, editor. Alan R. Liss, New York. 377–403.

Schulze, E., and M. Kirschner. 1988. New features of microtubule behaviour observed in vivo. *Nature.* 334:356–359.

Shelden, E., and P. Wadsworth. 1993. Observation and quantification of individual microtubule behavior in vivo: microtubule dynamics are cell-type specific. *J. Cell Biol.* 120:935–945.

Simon, J. R., S. F. Parsons, and E. D. Salmon. 1992. Buffer conditions and non-tubulin factors critically affect the microtubule dynamic instability of sea urchin egg tubulin. *Cell Motil. Cytoskel.* 21:1–14.

Simon, J. R., and E. D. Salmon. 1990. The structure of microtubule ends during the elongation and shortening phases of dynamic instability examined by negative-stain electron microscopy. *J. Cell Sci.* 96: 571–582.

Skibbens, R. V., V. P. Skeen, and E. D. Salmon. 1993. Directional instability of kinetochore motility during chromosome congression and segregation in mitotic newt lung cells: a push-pull mechanism. *J. Cell Biol.* 122:859–875.

Tabony, J. 1994. Morphological bifurcations involving reaction-diffusion processes during microtubule formation. *Science.* 264:245–248.

Vandecandelaere, A., S. R. Martin, and P. M. Bayley. 1995. Regulation of microtubule dynamic instability by tubulin-GDP. *Biochemistry.* 34: 1332–1343.

Vasquez, R. J., D. L. Gard, and L. Cassimeris. 1994. XMAP from *Xenopus*

eggs promotes rapid plus end assembly of microtubules and rapid microtubule polymer turnover. *J. Cell Biol.* 127:985–993.

Verde, F., M. Dogterom, E. Stelzer, E. Karsenti, and S. Leibler. 1992. Control of microtubule dynamics and length by cyclin A- and cyclin B-dependent kinases in *Xenopus* egg extracts. *J. Cell Biol.* 118: 1097–1108.

Walker, R. A., E. T. O'Brien, N. K. Pryer, M. F. Soboeiro, W. A. Voter, H. P. Erickson, and E. D. Salmon. 1988. Dynamic instability of individual microtubules analyzed by video light microscopy: rate constants and transition frequencies. *J. Cell Biol.* 107:1437–1448.

Wilson, L., and M. A. Jordan. 1994. Pharmacological probes of microtubule function. *In* Microtubules. J. S. Hyams and C. W. Lloyd, editors. Wiley-Liss, New York. 59–83.

Yamada, K. M., B. S. Spooner, and N. K. Wessells. 1971. Ultrastructure and function of growth cones and axons of cultured nerve cells. *J. Cell Biol.* 49:614–635.

Zimmerman, S. B., and A. P. Minton. 1993. Macromolecular crowding: biochemical, biophysical, and physiological consequences. *Annu. Rev. Biophys. Biomol. Struct.* 22:27–65.